Organic & Biomolecular Chemistry

PAPER

View Article Online
View Journal

Cite this: DOI: 10.1039/c6ob01163b

Chemical synthesis and enzymatic properties of RNase A analogues designed to enhance second-step catalytic activity†

David J. Boerema,*[a] Valentina A. Tereshko,[b] Junliang Zhang[c] and Stephen B. H. Kent[c]

Received 28th May 2016,
Accepted 23rd August 2016

DOI: 10.1039/c6ob01163b

www.rsc.org/obc

In this paper, we have used total chemical synthesis of RNase A analogues in order to probe the molecular basis of enzyme catalysis. Our goal was to obligately fill the adenine-binding pocket on the enzyme molecule, and to thus pre-orient the imidazole side chain of His^{119} in its catalytically productive orientation. Two designed analogues of the RNase A protein molecule that contained an adenine moiety covalently bound to distinct amino acid side chains adjacent to the adenine binding pocket were prepared. A crystal structure of one analogue was determined at 2.3 Å resolution. Kinetic data for RNA transphosporylation and 2′,3′ cyclic mononucleotide hydrolysis were acquired for the adenine-containing RNase A analogue proteins. As anticipated, the presence of a covalently attached adenine on the enzyme molecule *decreased* the rate of transphosphorylation and *increased* the rate of hydrolysis, although the magnitude of the effects was small. This work illustrates the use of total protein synthesis to investigate the chemistry of enzyme catalysis in ways not possible through traditional biochemistry or molecular biology.

The enzyme bovine pancreatic ribonuclease A (RNase A) is a small protein that catalyzes the cleavage and hydrolysis of single-stranded RNA.[1] The reaction is a two step process, in which two histidine residues (His^{12} and His^{119}) play catalytically essential roles. In the first step, the imidazole side chain of His^{12} acts as a general base to catalyze the intramolecular attack of a 2′-OH on the phosphodiester bond on the same ribose, while the imidazolium side chain of His^{119} acts as a general acid to protonate the 5′-OH leaving group on the next ribose moiety of the substrate.[2] The resulting terminal 2′,3′-phosphodiester cyclic nucleotide-containing fragment is released from the RNase A protein.[3] In the second step, the cyclic 2′,3′-phosphodiester is re-bound to the enzyme and is hydrolyzed to give a 3′-monophosphate final product (Scheme 1). In this second RNase A-catalyzed reaction, the roles of the two His side chains are reversed: the imidazole side chain of His^{119} acts as a general base to catalyze the attack of a water molecule on the cyclic 2′,3′-phosphodiester, while the imidazolium side chain of His^{12} acts as a general acid to protonate the 2′-OH leaving group in the substrate.[2]

Studies of the non-enzyme catalysed hydrolysis rates of small molecule linear and cyclic phosphodiesters have shown that the cyclic molecule is hydrolyzed at rates 10^6–10^8 times faster than the linear molecule.[4] This increase in rate appears to be due to either ring strain[5] or solvent effects.[6] In the RNase A catalyzed reaction, calculations by Thompson, *et al.*,[7] suggest that the intrinsic kinetic barrier for the cleavage of a P–O5′ bond in RNA is almost the same as the hydrolysis of a P–O2′ bond in a cyclic 2′,3′-phosphodiester. Yet, despite the fact that the two enzyme-catalyzed reactions are mechanistically almost identical, RNase A accelerates the rate of the first (transphosphorylation) step over 1000-times more effectively than the second (hydrolysis) step.[8]

Crystal structures of the 'empty' RNase A protein molecule, *i.e.* not bound to substrate analogues (Fig. 1(a)), showed that the side chain of histidine 119 can occupy two distinct conformations related by rotations around the Cα–Cβ and Cβ–Cγ bonds.[9] Of these two distinct His^{119} side chain conformations, only one is thought to be catalytically relevant to both steps of RNase A catalysis.[10]

The simplest RNA substrate cleaved by RNase A is the dinucleotide CpA. This substrate takes into account the preference of RNase A for a pyrimidine (in this case cytosine) on the 5′ side of the scissile bond and an adenine on the 3′ side. An X-ray crystal structure of RNase A containing a non-reactive analogue of this substrate, the deoxy-dinucleotide d(CpA) lacking the 2′-hydroxyl needed for transphosphorylation, has

[a]Department of Biochemistry & Molecular Biology, University of Chicago, Chicago, Illinois, USA. E-mail: dboerema@gmail.com
[b]Institute for Biophysical Dynamics, University of Chicago, Chicago, Illinois, USA
[c]Department of Chemistry, University of Chicago, Chicago, Illinois, USA
†Electronic supplementary information (ESI) available. See DOI: 10.1039/c6ob01163b

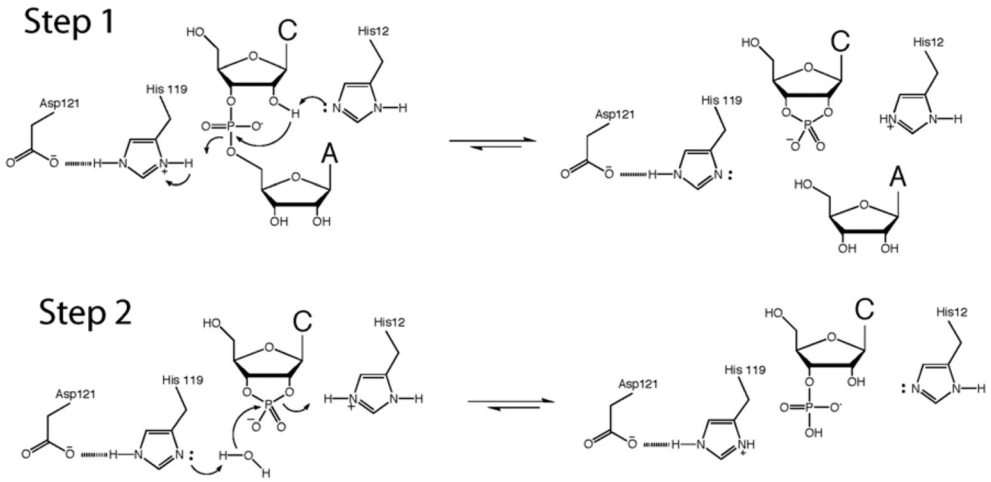

Scheme 1 The generally accepted mechanism of RNA phosphodiester bond cleavage/hydrolysis in a dinucleotide substrate by RNase A showing the role of the two main catalytic residues, histines 12 and 119.[2] The side chain imidazoles of these two histidine residues act alternately as general acids and bases. The 2′,3′-cyclic phosphodiester product is released into solution after the first step. When most of the initial substrate has been transphosphorylated the 2′,3′-cyclic phosphodiester product is rebound and hydrolyzed.[3]

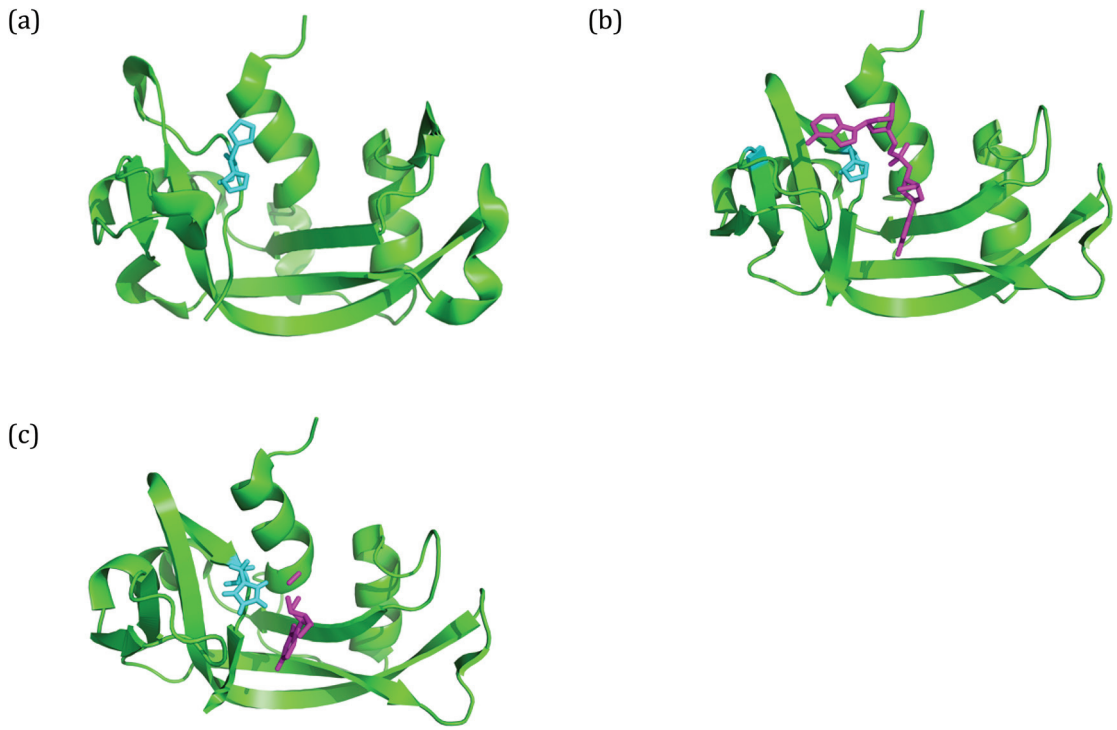

Fig. 1 X-ray structures of RNase A, with His^{119} side chain in cyan. (a) 'Empty' unliganded enzyme [PDB ID: 3RN3]; (b) RNase A bound to the dinucleotide d(CpA) (magenta) [PDB ID: 1RPG]; (c) RNase A bound to uridine vanidate (magenta) [PDB ID: 1RUV].

been solved (Fig. 1(b)) and can be used to explore the interactions of the enzyme with an adenine-containing substrate. Examination of the structure of RNase A bound to d(CpA) shows the *catalytically active* conformation of the histidine 119 side chain that is adopted during the Step 1 transphosphorylation reaction (Fig. 2(a)). The presence of the substrate adenine moiety bound in the B2 subsite (first base binding site 3′ to the scissile bond) prevents the histidine 119 side chain from accessing an inactive conformation.

Similarly, the structure of RNase A bound to uridine vanidate,[11,12] a so-called 'transition state analogue' for the Step 2 reaction, hydrolysis of a 2′,3′-cyclic phosphodiester, can be used to explore the interactions of the enzyme molecule with a second step substrate analogue [Fig. 1(c)]. During this second

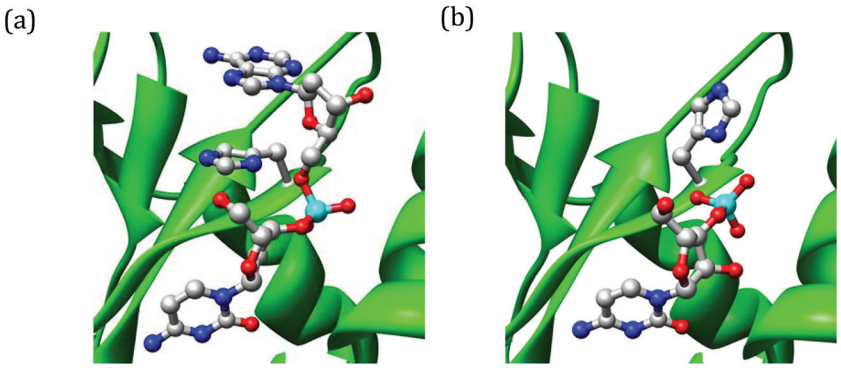

Fig. 2 Close-ups of the His^{119} side chain in distinct RNase A complexes. (a) RNase A bound to the Step 1 substrate analogue d(CpA) [PDB ID: 1RPG]; the His^{119} imidazole side chain is constrained in the catalytically productive orientation by the adenine moiety; (b) RNase A bound to the Step 2 product 3′CMP [PDB ID: 1RPF]; in the absence of adenine in subsite B2, the His^{119} imidazole side chain is not constrained and adopts a different conformation.

RNase A catalyzed reaction, the B2 subsite is not occupied by an adenine moiety, and is empty except for a few solvent molecules which form hydrogen bonds with asparagine 71 and other nearby side chains. Yet, in the complex with the transition state analogue uridine vanidate, the histidine 119 side chain imidazole is seen in its catalytically active conformation [Fig. 1(c)]. This observation suggests that in the Step 2 reaction, other His^{119} side chain conformations [see Fig. 2(b)] that are accessible because the adenine-binding pocket is empty, would not be catalytically effective. That idea is reinforced by a number of reports which suggest that filling the adenine binding pocket by adding exogenous adenine-containing small molecules can increase the rate of the RNase A catalyzed hydrolysis reaction by several fold.[13]

In the work reported here, we set out to investigate the effect of the histidine 119 side chain conformation on the rate of RNase A catalyzed hydrolysis of a 2′,3′-cyclic nucleotide. Our goal was to design and prepare a non-natural variant of RNase A with the side chain of histidine 119 pre-positioned in the catalytically relevant conformation for hydrolysis of a 2′,3′-cyclic nucleotide. The idea was to anchor an adenine moiety to the enzyme molecule itself, in the B2 subsite of the RNase A protein. Covalent attachment of the adenine ring to one of the residues making up the adenine binding pocket would be expected to keep the His^{119} side chain in its catalytically relevant conformation, and to thus speed up the RNase A catalyzed hydrolysis of a 2′,3′-cyclic nucleotide.

Results and discussion

Design

Analysis of the RNase A protein molecule bound to an inactive substrate analogue d(CpA) illustrates the interactions involved when the enzyme binds to polynucleotide substrates. The d(CpA) substrate analogue binds in a cleft on the surface of the enzyme with the phosphodiester bond located between the two catalytic histidine residues [Fig. 1(b)]. The adenine ring is held in a shallow binding pocket on the surface of the protein molecule by hydrogen bonds, primarily with the side chain of asparagine 71. In this conformation, the histidine 119 side chain also forms a hydrogen bond with the side chain of aspartic acid 121. These interactions (along with the side chain of glutamine 111) make up the adenine binding pocket, referred to as the B2 subsite (so called because it is the second base binding site) on the RNase A protein molecule. The planes formed by the imidazole ring in the side chain of histidine 119 and the adenine ring are essentially parallel, and the His^{119} imidazole moiety has direct access to the scissile bond [Fig. 2(a)]. Shielding of the His^{119} side chain from the aqueous solvent by the adenine will also influence the properties of the catalytic imidazole. When the d(CpA) substrate analogue is bound to the RNase A molecule, the His^{119} side chain imidazole is unable to occupy the second, *inactive* conformation, in which it would sterically clash with the adenine ring [compare Fig. 2(a) and (b)].

A suitable position for covalent attachment of an adenine moiety to the RNase A protein molecule was at asparagine 71. The side chain carboxamide moiety of asparagine 71 forms two hydrogen bonds to two different nitrogen atoms on the adenine ring when d(CpA) is bound in the B2 subsite of the RNase A protein molecule (Fig. 3). An adenine attached to a Lys residue at position 71 could be modeled to reach and occupy the B2 subsite, and would thus be expected to

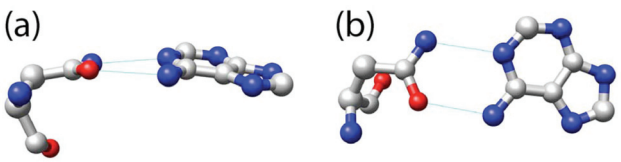

Fig. 3 A close up view of the interaction between the asparagine-71 side chain and the adenine ring in the adenine binding pocket from (a) the side and (b) the top. This figure was drawn from coordinates with PDB ID 1RPG.[14]

constrain the side chain imidazole of His^{119} in its catalytically active conformation.

Another candidate for covalent attachment of an adenine moiety was residue alanine 109 which is located on the β-strand adjacent to the β-strand containing His^{119}, with its side chain pointing towards, but not extending into, the adenine binding pocket. We hypothesized that an adenine moiety attached through just two methylenes to the side chain of an amino acid at position 109 would have less conformational flexibility and thus be more effective at occupying the B2 subsite. Such an analogue located at residue 109 would also leave the Asn^{71} side chain intact, so that the carboxamide moiety is able to form H-bonds to the adenine and orient it in the binding pocket (Fig. 3).

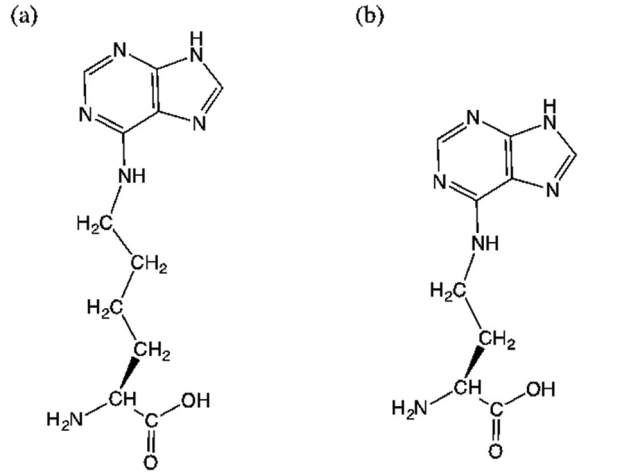

Fig. 4 Structures of the two unnatural amino acids designed to covalently fix an adenine in the adenine-binding pocket (subsite B2) of the RNase A enzyme molecule. (a) Lys(Ade), designed to replace asparagine 71. (b) Dab(Ade), designed to replace alanine 109.

Synthesis

Two non-natural amino acids were designed containing covalently linked adenine moieties attached through the two different length side chains [referred to as Lys(Ade) and Dab (Ade)] (Fig. 4) and were prepared in suitably protected form as described in Fig. 5.

Each of these adenine-containing amino acids was incorporated into a separate preparation of the [D83A]RNase A enzyme molecule at positions 71 and 109 respectively, using the previously reported synthetic approach.[15] The enzyme [D83A]RNase A itself was also synthesized as a control. Analytical characterization of the resulting purified synthetic enzymes, [N71 K(Ade), D83A] and [D83A, A109Dab(Ade)]RNase A, are shown in Fig. 6.

Enzyme kinetics

These synthetic adenine-containing RNase A protein molecules were expected to be enzymatically active, but to have an *increased* rate for the *hydrolysis reaction* due to an increased occupancy of the catalytically-productive conformation of the His^{119} side chain imidazole, and to have a *decreased* rate for the *transphosphorylation reaction* due to (partial) blocking of the adenine binding pocket needed to bind the polynucleotide substrate.

Steady-state kinetic parameters for the transphosphorylation of polycytidylic acid [poly(C)], and for the hydrolysis of

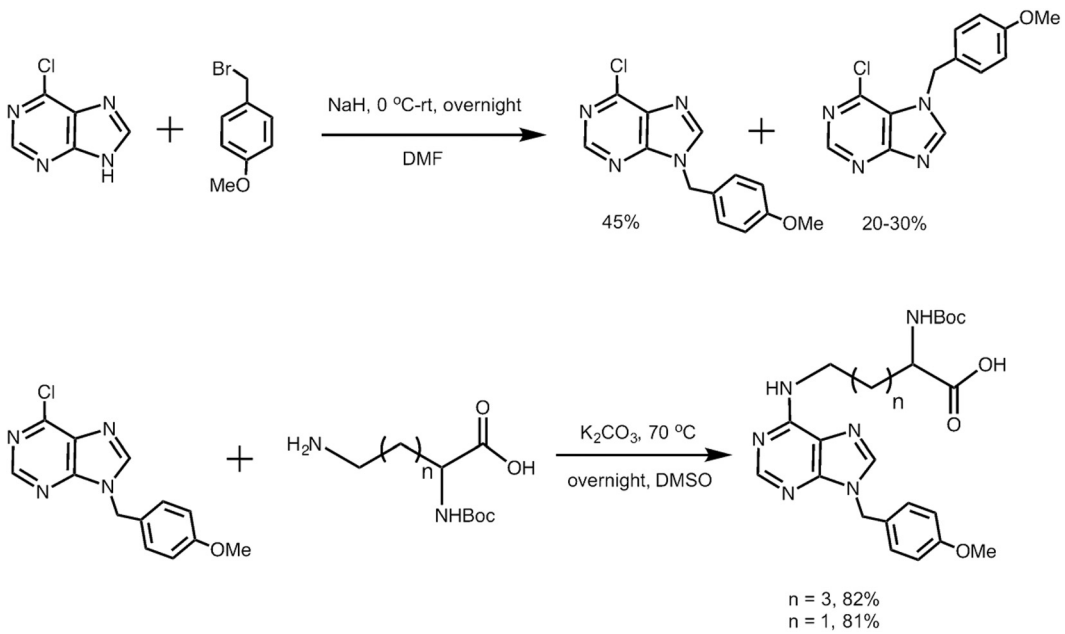

Fig. 5 General synthetic scheme for the preparation of the protected adenine-containing amino acids. Full details are given in Experimental methods.

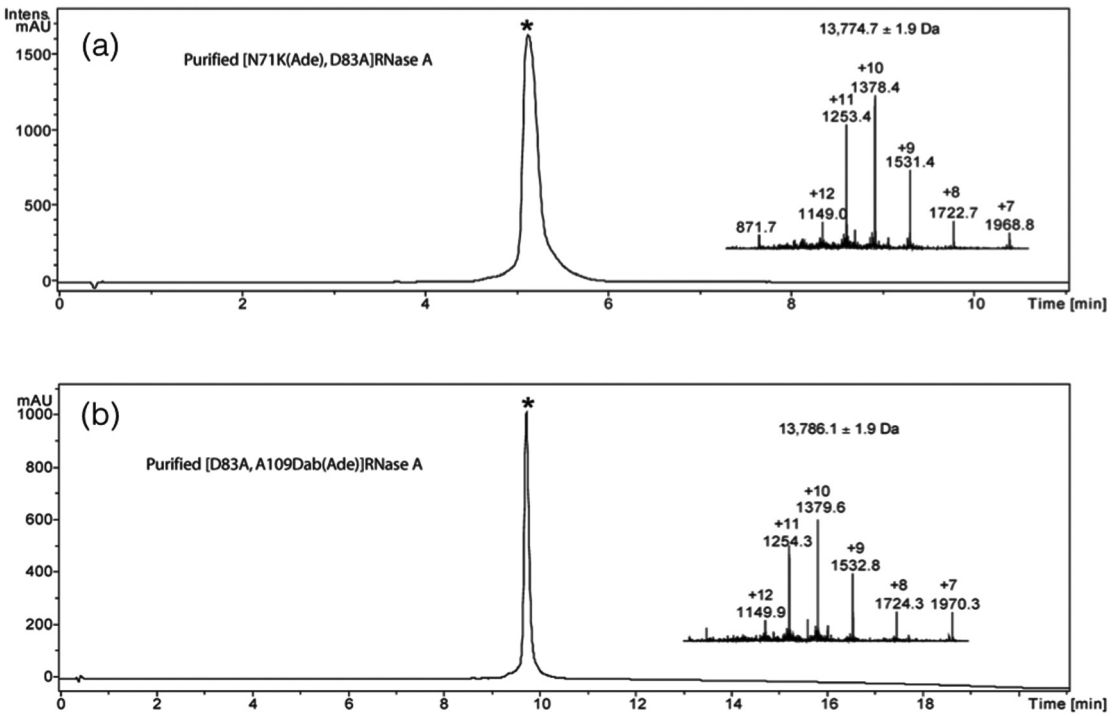

Fig. 6 LC/MS analysis of the two synthetic non-natural RNase A enzyme analogues. (a) [N71 K(Ade), D83A]RNase A. (b) [D83A, A109Dab(Ade)]RNase A. Note the different time scales for panels (a) and (b). For each panel, the inset electrospray mass spectrum was taken across entire peak labeled with an asterisk. Theoretical masses (average isotope composition) are: [N71 K(Ade), D83A]RNase A 13770.3 Da; [D83A, A109Dab(Ade)]RNase A 13785.8 Da.

cytidine 2′,3′-cyclic monophosphate (C>p) were determined for each of the non-natural synthetic enzyme molecule analogues. The data are shown in Table 1 along with data for the same reaction catalyzed by the previously characterized [D83A]RNase A as a control.

The rate of C>p hydrolysis by [N71 K(Ade), D83A]RNase A was 4-fold *greater* than synthetic [D83A]RNase A, somewhat larger than the 2–3 fold rate increases resulting from the addition of adenine-containing small molecules to the reaction.[13] This suggests that the covalently attached adenine is affecting the enzyme mechanism in a similar manner to exogenous adenine bound in the adenine binding pocket, presumably orienting the histidine 119 side chain to some extent. The relatively small 1.8 fold *decrease* in the rate of poly(C) transphosphorylation suggests that the polynucleotide substrate is not blocked from binding to the active site as predicted. Instead, this slight decrease is more consistent with the rate decrease expected for the deletion of the Asn^{71} side chain-substrate hydrogen bonding interaction for an all cystosine-containing polynucleotide substrate.[16]

Conversely, the more conformationally restricted adenine-containing side chain [D83A, A109Dab(Ade)]RNase A analogue showed a 1.9 fold *increase* in the rate of C>p hydrolysis, a smaller than expected rate enhancement, and a 16 fold *decrease* in the rate of poly(C) transphosphorylation that was more in line with the decrease predicted.

Table 1 Comparison of the measured steady state kinetic parameters for the Step 1 reaction, transphosphorylation of poly(C), and the Step 2 reaction, hydrolysis of C>p, by unmodified synthetic [D83A]RNase A and by the synthetic adenine-containing enzyme molecules [N71 K(Ade), D83A] RNase A and [D83A, A109Dab(Ade)]RNase A. Assays were performed at 25 °C in 0.1 M MES/NaOH pH 6.00 containing NaCl (0.1 M). Reactions were monitored at 250 nm [poly(C) transphosphorylation] and 290 nm (C>p hydrolysis)

RNase A	Substrate	k_{cat} (s^{-1})	K_m (μM)	k_{cat}/K_m ($\times 10^6$ M^{-1} s^{-1})
Synthetic [D83A][a]	Poly(C)	198 ± 3	5.1 ± 0.5	39 ± 4
	C>p	2.0 ± 0.07	285 ± 20	0.0070 ± 0.0006
Synthetic [N71 K(Ade), D83A]	Poly(C)	110 ± 3	26 ± 2	4.23 ± 0.12
	C>p	9.24 ± 0.02	460 ± 20	0.0201 ± 0.0008
Synthetic [D83A, A109Dab(Ade)]	Poly(C)	12.2 ± 0.2	4.4 ± 0.4	2.8 ± 0.3
	C>p	3.74 ± 0.10	470 ± 30	0.008 ± 0.0006

[a] Data for synthetic [D83A]RNase A taken from ref. 15.

The presence of a covalently bound adenine moiety had varying effects on the K_m of the reaction with poly(C) depending on where it was attached. For [N71 K(Ade), D83A]RNase A the K_m for the reaction with poly(C) is elevated ~5× indicating that poly(C) does not bind as tightly as in the D83A enzyme. This is likely a result of the modification made directly in the active/binding site, and the direct replacement of a B2 binding site residue. The K(Ade)71 side chain likely interferes somewhat with the binding of the poly(C) molecule. For [D83A, A109Dab(Ade)]RNase A, the K_m of the reaction with poly(C) is virtually unchanged indicating little to no perturbation of the association rate between poly(C) and the enzyme. This could be explained by the attachment of the Ade sidechain OUTSIDE of the binding pocket. It may be easier for the poly(C) to displace the Ade without overly-disrupting the rest of the intact B2 subsite.

For the Step 2 reaction, both modifications of RNase A had a similar impact on the K_m of the reaction (~1.5× increase in K_m). This indicates that both modifications decrease the binding affinity of the C>p substrate in a similar manner. Since the C>p reaction does not involve binding of the substrate to the B2 subsite, the specifics of the modification may have less direct effects on the substrate: enzyme interaction.

Crystal structure by X-ray diffraction

To further understand the kinetic data presented above, structural characterization of the chemically synthesized [N71 K(Ade), D83A]RNase A was undertaken. Crystals of [N71 K(Ade), D83A]RNase A were successfully grown and diffracted to a resolution of 2.3 Å. Diffraction statistics indexed the data in the *P*1 space group. The structure was solved by molecular replacement, using the structure of synthetic [D83A]RNase A [PDB ID 2NUI] as a search model. The resulting structure contained four copies of the RNase A analogue in the unit cell, providing four separate pictures of the histidine 119/Lys(Ade)71 interaction (Fig. 7).

In three of the molecules in the unit cell, the side chain of Lys(Ade)71 is involved in intermolecular contacts with RNase A molecules in neighboring unit cells [Fig. 8(a), (b) and (d)]. These interactions appear to stabilize the position of the non-natural side chain, resulting in the well-defined density that is observed. The fourth molecule lacks any interaction with neighboring RNase A molecules in the region of the non-natural Lys(Ade)71 side chain [Fig. 8(c)]. As a result, the side chain is disordered, and no density is observed in the final structure. Presumably this structure, with its lack of intermolecular contacts in the region of interest, is more representative of the molecule in solution, and indicates that the adenine-containing side chain exhibits significant freedom of movement. Despite this flexibility of the adenine-containing side chain, the histidine 119 side chain in this molecule appears to be almost exclusively in the active conformation [Fig. 8(c)]; it appears that the presence of the flexible side chain successfully alters the histidine 119 dynamics enough to increase the occupancy of the active conformation. If the enzyme analogue behaves in a similar manner in solution with the histidine 119 side chain dynamics altered to favor the active conformation, this observation may help explain the observed 4-fold increase in the rate of C>p hydrolysis by [N71 K(Ade), D83A]RNase A. In addition, the flexibility of the adenine-containing side chain may also help explain the lower then expected decrease in the rate of poly(C) transphosphorylation: the flexibility allows the adenine-containing side chain to diffuse out of the adenine binding pocket, allowing polynucleotide substrates to bind and undergo transphosphorylation at near-native rates.

Structural characterization by X-ray diffraction of the synthetic [D83A, A109Dab(Ade)] RNase A protein was also attempted, but in limited trials no crystals were obtained. Presumably, for this analogue the larger *decrease* in the observed rate of transphosphorylation reaction is the result of decreased flexibility of the shorter adenine-containing side chain, which should keep the adenine moiety in the adenine binding pocket and thus exclude the polynucleotide RNA substrate. Without further structural characterization it is difficult to explain the small difference in hydrolysis rates between the two RNase A protein analogues.

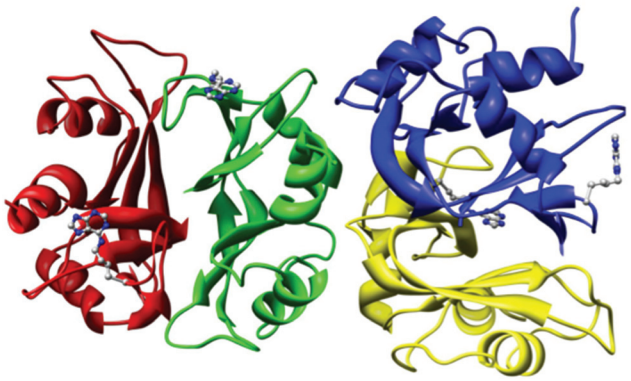

Fig. 7 Ribbon representation of the four molecules contained in the [N71 K(Ade), D83A]RNase A unit cell.

Summary and conclusions

Total synthesis of two chemical analogues of the RNase A protein molecule, each of which contained a covalently attached adenine moiety, was used to study the mechanism of enzyme catalysis in ways not readily accessible through traditional biochemistry or molecular biology. The results obtained demonstrate that the dynamics of the histidine 119 side chain are at least partially responsible for the much lower rate acceleration of the enzyme catalyzed Step 2 hydrolysis reaction in comparison to the Step 1 transphosphorylation reaction. Overall, the magnitudes of the effects of covalent adenine attachment to the enzyme protein molecule on the rates of the two reactions catalyzed by RNase A were modest, although they were in the expected directions: slowing the

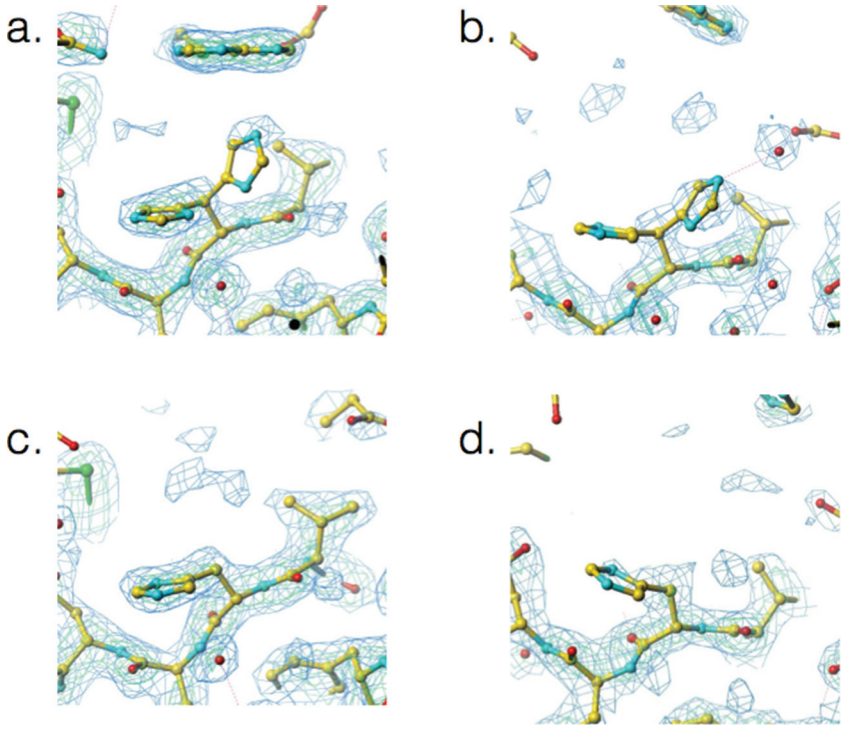

Fig. 8 Models of the histidine 119 side chain placed in the observed electron density in each of the four molecules seen in the unit cell of the [N71 K(Ade), D83A]RNase A crystal structure. (a) In molecule A the histidine 119 side chain primarily occupies the A conformation. The adenine ring can be seen at the top of the panel. (b) In molecule B there is weak density in the B conformation and even weaker density in the A conformation indicating disorder. A portion of the adenine ring can be seen at the top of the panel. (c) In molecule C, in which the adenine ring is disordered, the histidine 119 side chain appears well ordered in the A conformation. (d) In molecule D the density for the histidine 119 side chain is very weak, indicating a high degree of disorder for this side chain. A portion of the adenine ring can be seen at the top right of the panel. The outer electron density contours are drawn at 1σ.

transphosphorylation reaction; and speeding up the hydrolysis of a 2′,3′ cyclic mononucleotide. A more refined design of an unnatural RNase A protein with a rotationally immobilized His^{119} side chain and a locked/correctly oriented adenine in subsite B2 might add further insight to the role of this imidazole side chain in RNase A enzyme catalysis.

Experimental methods

Amino acid sequence of the RNase A polypeptide chain

```
1                                                   50
KETAAAKFER QHMDSSTSAA SSSNYCNQMM KSRNLTKDRC KPVNTFVHES
51                                                  100
LADVQAVCSQ KNVACKNGQT NCYQSYSTMS ITDCRETGSS KYPNCAYKTT
101                    124
QANKHIIVAC EGNPYVPVHF DASV
```

Amino acid sequence of the RNase A polypeptide chain.[17] The protein molecule contains eight cysteines, which form four disulfide bridges (Cys^{26}–Cys^{84}, Cys^{40}–Cys^{95}, Cys^{58}–Cys^{110}, Cys^{65}–Cys^{72}) in the native enzyme structure.

Materials

2-(1*H*-Benzotriazol-1-yl)-1,1,3,3-tetramethyuronium hexafluorophosphate (HBTU), *S*-trityl-mercaptopropionic acid, and Boc-amino acids were obtained from Peptides International, Louisville (Kentucky), except Boc-(4*R*)-1,3-thiazolidine-4-carboxylic acid (Boc-Thz) which was obtained from NovaBiochem, San Diego. Boc-aminoacyl-OCH_2-Pam-resins were obtained preloaded from Applied Biosystems, Foster City, or synthesized from Boc-L-aminoacyl-(4-carboxymethyl)benzyl esters (NeoMPS, San Diego) and aminomethyl-resin (Rapp Polymer, Germany) as described previously.[18] Side chain protecting groups used were: Arg(Tos), Asp(OcHex), Asn(Xan), Cys (4MeBzl), Glu(OcHex), His(DNP), His(Bom), Lys(2ClZ), Ser (Bzl), Thr(Bzl), and Tyr(BrZ). *N*,*N*-Diisoproylethylamine (DIEA) was obtained from Applied Biosystems, Foster City. *N*,*N*-Dimethylformamide (DMF), dichloromethane, and HPLC grade acetonitrile were purchased from VWR. Diethyl ether was purchased from Fisher. RNase-free buffer reagents (MES, NaCl, NaOH, and water) from Fisher were used in the kinetic assays. Trifluoroacetic acid (TFA) was obtained from Halocarbon Products, New Jersey. HF was purchased from Matheson Tri-Gas. Tris(2-carboxyethyl)phosphine hydrochloride (TCEP), *p*-cresol, triisopropylsilane, 4-mercaptophenylacetic acid (MPAA), polycytidylic acid [poly(C)], cytidine 2′,3′-cyclic phosphate (C>p), and native RNase A type XII-A were purchased from Sigma-Aldrich.

Preparation of Boc-Lys(AdeMeOBzl) and Boc-Dab(AdeMeOBzl)

9-(4′-Methoxybenzyl)-6-chloropurine was prepared according to a previously published literature procedure.[19]

Detailed procedures for the preparation of each modified amino acid are described below.

9-(4′-Methoxybenzyl)-purine-(6-N^{ω})-N^{α}-(*tert*-butoxylcarbonyl)-L-lysine. The mixture of 9-(4′-methoxybenzyl)-6-chloropurine (1.00 g, 3.65 mmol), N^{α}-(*tert*-butoxylcarbonyl)-L-lysine (0.75 g, 3.05 mmol) and K_2CO_3 (0.8 g) in 20 mL of DMSO was stirred at 70 °C overnight. 250 mL of water and 20 mL of saturated Na_2CO_3 were added and the aqueous solution was extracted with EtOAc three times, in order to remove the excess 9-benzyl-6-chloropurine. The pH of the aqueous layer was adjusted to 6–7 by 1 N HCl and then extracted with EtOAc or CH_2Cl_2. The combined organic layers were washed with water once and dried over $MgSO_4$. After filtration and removal of the solvent, 9-(4′-methoxybenzyl)-purine-(6-N^{ω})-N^{α}-(*tert*-butoxylcarbonyl)-L-lysine (1.20 g) was obtained in 82% yield. (If it contains some little impurity, impurity can be removed by addition of some mixture solution of EtOAc and hexanes in a ratio of 1 : 10 and filtration). ^{1}H NMR (500 MHz, $CDCl_3$) δ 9.57 (br, s, 0.30 H), 8.45 (s, 1 H), 8.10 (br, s, 0.20 H), 7.78 (br, s, 0.20 H), 7.64 (s, 1 H), 7.60 (br, s, 1 H), 7.23 (d, J = 8.0 Hz, 2 H), 6.86 (d, J = 8.0 Hz, 2 H), 5.65–5.50 (br, 1 H), 5.26 (s, 2 H), 4.33 (d, J = 6.5 Hz, 1 H); 3.78 (s, 3 H), 3.75 (br, s, 1 H), 3.48 (br, s, 1 H), 1.95 (br, s, 1 H), 1.85 (br, s, 1 H), 1.76 (s, 2 H), 1.70–1.50 (m, 2 H), 1.44 (s, 9 H); ^{13}C NMR [see Fig. S1†] (125 MHz, $CDCl_3$) δ 176.78, 159.58, 155.51, 154.35, 153.65, 148.29, 138.59, 129.40, 126.86, 117.88, 114.31, 79.37, 55.15, 53.69, 46.80, 40.42, 32.05, 28.53, 28.27, 22.70. LCMS data are given in Fig. S2.†

9-(4′-Methoxybenzyl)-purine-(6-N^{γ})-N^{α}-(*tert*-butoxylcarbonyl)-L-diaminobutyric acid. The reaction of 9-(4′-methoxybenzyl)-6-chloropurine (1.48 g, 5.40 mmol), N^{α}-(*tert*-butoxylcarbonyl)-L-2,4-diaminobutyric acid (1.09 g, 5.00 mmol) and K_2CO_3 (1.38 g) afforded 1.83 g (81%) of 9-(4′-methoxybenzyl)-purine-(6-N^{ω})-N^{α}-(*tert*-butoxylcarbonyl)-L-diaminobutyric acid. ^{1}H NMR (500 MHz, $CDCl_3$) δ 9.69 (br, s, 0.25 H), 8.42 (s, 1 H), 7.79 (br, s, 0.25 H), 7.60 (br, s, 0.25 H), 7.28 (s, 1 H), 7.18 (d, J = 8.0 Hz, 2 H), 6.85 (d, J = 8.0 Hz, 2 H), [6.22 (br, s, 0.33 H), 5.97 (br, s, 0.67 H)], [5.26 (br, s, 0.50 H), 5.08 (s, 1.50 H)], 4.44 (s, 1 H), 4.31 (0.25 H), 3.96 (br, s 1 H), 3.75 (s, 3 H), 3.65 (br, s, 1 H), 2.48 (br, s 1 H), 2.16 (br, s, 1 H), 1.44 (s, 9 H); ^{13}C NMR [see Fig. S3†] (125 MHz, $CDCl_3$) δ 176.44, 159.74, 155.56, 154.42, 153.38, 148.39, 138.52, 129.42, 126.87, 117.84, 114.43, 79.53, 55.24. LCMS data are given in Fig. S4.†

Peptide synthesis

Peptide-α*COSCH$_2$CH$_2$COLeu* (-αCOSR) thioesters were synthesized on a *HCOSCH$_2$CH$_2$COLeu-OCH$_2$*-Pam-resin, as described previously.[20] Arginine-tagged segment 65–83 was synthesized on Boc-Arg-*OCH$_2$*-Pam-resin to which six arginines and a thioester moiety were coupled. Peptides were synthesized on a 0.5 mmol scale, using the manual Boc chemistry "*in situ* neutralization"/HBTU protocol described previously.[21] After chain assembly was complete, the N^{α}-Boc group was removed with TFA, and the peptide-resin was washed with dichloromethane and dried by aspiration. The peptide was cleaved from the resin and the side-chain protecting groups were simultaneously removed by treatment with anhydrous HF at 0 °C for 1 hour, with 5–10% (v/v) *p*-cresol added as a scavenger. After thorough removal of HF by evaporation, the peptide was precipitated and washed with cold diethyl ether, dissolved in 50% aqueous acetonitrile + 0.1% TFA, and then lyophilized.

Peptide analysis and purification

Analytical reverse-phase HPLC was performed on an Agilent 1100 system with either a Microsorb C-18 (5 μm, 300 Å, 2.1 × 50 mm) silica column packed in-house or a Vydac C-4 (5 μm, 300 Å, 2.1 × 50 mm) silica column. Peptide masses were obtained using on-line electrospray MS detection. Preparative HPLC was performed on C-4 and C-18 (10 × 250, 22 × 250, 50 × 250 mm) columns from Vydac, depending on the peptide quantities and retention characteristics. Peptides were eluted from the column using an appropriate shallow gradient of acetonitrile/0.08% TFA *versus* water/0.1% TFA. Fractions containing the desired purified product were identified by analytical LC-MS, then combined and lyophilized.

Synthesis of RNase A analogues by native chemical ligation

The synthesis of the full length 124 amino acid polypeptide chains of the RNase A analogues were performed using two sets of sequential one-pot ligations similar to that described previously.[16] Briefly, equimolar amounts of purified, lyophilized RNase A(95-124) and RNase A(Thz^{84}-94)-αCOSR were dissolved to a concentration of approximately 4 mM in 6 M guanidine hydrochloride, 0.1 M Na phosphate pH 7.0 containing 200 mM MPAA and 20 mM TCEP (ligation buffer). Upon reaction completion, the Thz was converted to cysteine by addition of 0.2 M methoxylamine HCl, adjustment of pH to 4.0, and overnight reaction. The next ligation was performed by re-adjusting to pH 7.0, adding 1.3 equivalents of [D83A]RNase A(Thz^{65}-83)-αCOSR′ (containing a C-terminal 6-Arg tag in the thioester leaving group and one of the described un-natural amino acids) and adding an additional 20 mM TCEP. Following completion of the ligation reaction, the Thz protection was removed overnight by lowering the pH of the reaction to 4.0 *without additional methoxylamine HCl*. The product, polypeptide RNase A(65-124), containing one of the two described unnatural amino acids, was purified by preparative HPLC.

The second series of one-pot ligations was initiated by dissolving RNase A(65-124) containing one of the modified amino acids and RNase A(Thz^{40}-64)-αCOSR to approximately 2.5 mM in 0.1 M sodium phosphate pH 7.0 ligation buffer containing 200 mM MPAA and 20 mM TCEP. After the reaction was complete, Thz deprotection was performed overnight by adding 0.2 M methoxylamine HCl at pH 4.0 as described above. The ligation of RNase A(Thz^{26}-39)-αCOSR was initiated by re-adjusting the reaction pH to 7.0, adding the peptide, and an additional 20 mM TCEP. After the reaction was complete,

Thz deprotection was performed overnight by lowering the pH of the reaction to 4.0. The final ligation was initiated by re-adjusting the reaction solution to pH 7.0 and adding RNase A(1-25)-αCOSR and an additional 20 mM TCEP. The full length product [D83A]RNase A(1-124) polypeptide containing one of the modified amino acids was purified from the completed ligation reaction by preparative HPLC.

Folding the RNase A analogues

Purified [D83A]RNase A(1-124) containing one of the modified amino acids was dissolved in 6 M guanidine HCl, 0.1 M Tris pH 8.0 to a concentration of approximately 0.5 mM (6.8 mg mL^{-1}). This solution was diluted with a buffered solution containing cysteine and cystine to final concentrations of 0.5 M guanidine HCl, 0.1 M Tris pH 8.0, 8 mM cysteine, 1 mM cystine, and 0.04 mM (0.57 mg mL^{-1}) [D83A]RNase A(1-124) containing one of the modified amino acids, and was stirred for approximately 8 h. The reaction was monitored by analytical LC-MS. Folded enzyme protein molecule was purified from the folding reaction by preparative HPLC, and was characterized by LC-MS.

BCA protein assay

Concentrations of the modified enzyme molecules were determined using a BCA Protein Assay Kit purchased from Pierce (Rockford, IL). The assay was performed according to the manufacturers directions using a solution of RNase A of known concentration (determined from absorbance at 277.5 nm) to construct a standard curve. The result of the assay for the synthetic proteins was compared to the standard curve to determine concentrations of the two RNase A analogues.

Kinetic assays of RNase A analogues

All kinetics measurements were carried out on an Agilent 8453 UV-Vis diode array spectrophotometer. Initial velocities were determined using the manufacturer-supplied ChemStation software. Enzymes were dissolved in 10 mM MES/NaOH buffer, pH 6.0; NaCl was dialyzed in to a concentration of 100 mM and the final solutions were filtered with a 0.2 μm nylon syringe filter.

First step assay. Steady state kinetic parameters for the cleavage of poly(C) were determined using the procedures and extinction coefficients reported previously.[22] Poly(C) was obtained from Sigma-Aldrich and was purified by precipitation from aqueous ethanol (70% v/v) before use. Assays were preformed at 25 °C in 0.1 M MES/NaOH pH 6.00 containing NaCl (0.1 M), substrate (3.8–130 μm), and enzyme (4.8–5 nM) and monitored at 250 nm. The values of k_{cat}, K_m, and k_{cat}/K_m were determined from initial velocity data using the Enzyme Kinetics extension of SigmaPlot 9.0 (Systat Software Inc.).

Second step assay. Steady state kinetic parameters for the hydrolysis of 2′3′C>p were determined using a modification of the procedures previously reported.[23] Assays were performed at 25 °C in 0.1 M MES/NaOH pH 6.00 containing NaCl (0.1 M), substrate (75 μm–1.5 mM), and enzyme (410–730 nM) and monitored at 290 nm. The measured $\Delta\varepsilon$ coefficient for this reaction was 792 M^{-1} cm^{-1} at 290 nm. The values of k_{cat}, K_m, and k_{cat}/K_m were determined from initial velocity data using the Enzyme Kinetics extension of SigmaPlot 9.0 (Systat Software Inc.).

Crystallization, X-ray data collection, and refinement statistics for synthetic [N71 K(Ade), D83A]RNase A

[N71 K(Ade), D83A]RNase A enzyme solution for crystallization was made by dissolving enzyme to final concentrations of 10–20 mg mL^{-1} in de-ionized water. Crystals were grown using hanging drop vapor diffusion methods. [N71 K(Ade), D83A] RNase A crystals were obtained from drops consisting of 2 μL enzyme solution and 2 μL crystallization solution. The crystallization solution used for synthetic [N71 K(Ade), D83A]RNase A was made by mixing Hampton Index Reagents 3 and 9 (Hampton Research, Aliso Viejo, CA) in a 1 : 1 ratio. The resulting solution was 0.1 M bis–tris, 1.0 M ammonium sulfate, 1.5 M NaCl, with a pH of 5.89. Crystals of synthetic [N71 K(Ade), D83A]RNase A formed within two days. The enzyme molecule crystallized in the *P*1 space group. For low temperature data collection, crystals were transferred to the cryoprotectant (paraffin oil) for a few seconds and flash-frozen

Table 2 Data collection and refinement statistics for synthetic [N71 K(Ade), D83A]RNase A

	Synthetic [N71 K(Ade), D83A] RNase A
Data collection	
Space group	*P*1
Cell dimensions	
a (Å)	37.58
b (Å)	50.53
c (Å)	62.86
α (°)	85.26
β (°)	71.31
γ (°)	82.70
Resolution[a] (Å)	50–2.3 (2.38–2.30)
R_{merge}	0.136 (0.284)
$I/\sigma I$	10.4(4.0)
Completeness, %	97.7 (all)
1.18–1.13 Å	
1.13–1.09 Å	
1.09–1.05 Å	
Redundancy	1.9(1.9)
Refinement	
Resolution (Å)	60.41–2.30
No. reflections	
Work/free set	17 162/1960
R_{work}/R_{free}	22.3/29.1
No. residues	
Protein	496
Chloride	0
Bis–tris	0
Water	98
B-factor ($Å^2$)	14.928
R.m.s. deviations	
Bond lengths (Å)	0.008
Bond angles (°)	1.14

[a] Highest resolution shell is shown in parenthesis.

in liquid nitrogen. X-ray data were collected using 1° oscillation width at SerCAT station 22ID (λ = 0.97985 Å, 10 second exposure time) at the Advance Photon Source (APS), Argonne, Illinois. Images were processed and scaled with HKL2000.[24] The structure was solved by molecular replacement using MOLREP[25] with the [D83A]RNase A structure previously determined [PDB ID 2NUI] as a starting model (Table 2). The rigid body refinement, restrained positional and anisotropic temperature factor refinement, as well as search for water molecules, were carried out in REFMAC5 implemented in CCP4.[25] A Ramachandran plot calculated with PROCHECK[26] indicated that 100% of the non-Gly and non-Pro residues in the final models lie in the most favored and additional allowed regions. The SigmaA-weighted 2Fo-Fc and Fo-Fc Fourier maps were calculated in CCP4. The Fourier maps were displayed and examined in TURBO-FRODO.[27] Alignment of the two structures was performed with CCP4. Figures showing the electron maps and three-dimensional structures were prepared using TURBO-FRODO and the UCSF Chimera package,[28] respectively. The coordinates and structure factors have been deposited in the Protein Data Bank with PDB ID 2OQF.

References

1 C. M. Cuchillo, M. V. Nogués and R. T. Raines, Bovine Pancreatic Ribonuclease: Fifty Years of the First Enzymatic Reaction Mechanism, *Biochemistry*, 2011, **50**, 7835–7841.
2 R. T. Raines, Ribonuclease A, *Chem. Rev.*, 1998, **98**(3), 1045–1066.
3 C. M. Cuchillo, X. Parés, A. Guasch, T. Barman, F. Travers and M. Nogués, The role of 2′,3′-cyclic phosphodiesters in the bovine pancreatic ribonuclease A catalysed cleavage of RNA: intermediates or products?, *FEBS Lett.*, 1993, **333**(3), 207–210.
4 P. C. Haake and F. H. Westheimer, Hydrolysis and Exchange in Esters of Phosphoric Acid, *J. Am. Chem. Soc.*, 1961, **83**(5), 1102–1109.
5 R. Kluger and S. D. Taylor, On the origins of enhanced reactivity of five-membered cyclic phosphate esters. The relative contributions of enthalpic and entropic factors, *J. Am. Chem. Soc.*, 1990, **112**(18), 6669–6671.
6 A. Dejaegere and M. Karplus, Hydrolysis rate difference between cyclic and acyclic phosphate esters: solvation versus strain, *J. Am. Chem. Soc.*, 1993, **115**(12), 5316–5317.
7 J. E. Thompson, T. G. Kutateladze, M. C. Schuster, F. D. Venegas, J. M. Messmore and R. T. Raines, Limits to catalysis by ribonuclease A, *Bioorg. Chem.*, 1995, **23**(4), 471–481.
8 J. E. Thompson, F. D. Venegas and R. T. Raines, Energetics of Catalysis by Ribonucleases: Fate of the 2′,3′-Cyclic Phosphodiester Intermediate, *Biochemistry*, 1994, **33**(23), 7408–7414.
9 B. Howlin, D. S. Moss and G. W. Harris, Segmented anisotropic refinement of bovine ribonuclease A by the application of the rigid-body TLS model, *Acta Crystallogr., Sect. A: Fundam. Crystallogr.*, 1989, **45**(12), 851–861.
10 J. de Mel, V. Srini, M. S. Doscher, P. D. Martin and B. F. Edwards, The occupancy of two distinct conformations by active-site histidine-119 in crystals of ribonuclease is modulated by pH, *FEBS Lett.*, 1994, **349**(1), 155–160.
11 J. E. Ladner, B. D. Wladkowski, L. A. Svensson, L. Sjölin and G. L. Gilliland, X-ray structure of a ribonuclease A–uridine vanadate complex at 1.3 Å resolution, *Acta Crystallogr., Sect. D: Biol. Crystallogr.*, 1997, **53**(3), 290–301.
12 A. Wlodawer, M. Miller and L. Sjölin, Active site of RNase: neutron diffraction study of a complex with uridine vanadate, a transition-state analog, *Proc. Natl. Acad. Sci. U. S. A.*, 1983, **80**(12), 3628–3631.
13 (*a*) H. J. Wieker and H. Witzel, Zum Mechanismus der Ribonuclease-Reaktion, *Eur. J. Biochem.*, 1967, **1**, 251–258; (*b*) P. H. Haffner and J. H. Wang, Chemical kinetic and proton magnetic resonance studies of 5′-adenosine monophosphate binding to ribonuclease A, *Biochemistry*, 1973, **12**(8), 1608–1618; (*c*) M. Moussaoui, M. V. Nogués, A. Guasch, T. Barman, F. Travers and C. M. Cuchillo, The subsites structure of bovine pancreatic ribonuclease A accounts for the abnormal kinetic behavior with cytidine 2′, 3′-cyclic phosphate, *J. Biol. Chem.*, 1998, **273**(40), 25565–25572.
14 I. Zegers, D. Maes, M. H. Dao-Thi, L. Wyns, F. Poortmans and R. Palmer, The structures of RNase A complexed with 3′-CMP and d (CpA): active site conformation and conserved water molecules, *Protein Sci.*, 1994, **3**(12), 2322–2339.
15 D. J. Boerema, V. A. Tereshko and S. B. Kent, Total synthesis by modern chemical ligation methods and high resolution (1.1 Å) X-ray structure of ribonuclease A, *Pept. Sci.*, 2008, **90**(3), 278–286.
16 A. Tarragona-Fiol, H. J. Eggelte, S. Harbron, E. Sanchez, C. J. Taylorson, J. M. Ward and B. R. Rabin, Identification by site-directed mutagenesis of amino acids in the subsite of bovine pancreatic ribonuclease A, *Protein Eng.*, 1993, **6**(8), 901–906.
17 D. G. Smyth, W. H. Stein and S. Moore, The sequence of amino acid residues in bovine pancreatic ribonuclease: revisions and confirmations, *J. Biol. Chem.*, 1963, **238**(1), 227–234.
18 A. R. Mitchell, S. B. Kent, M. Engelhard and R. B. Merrifield, A new synthetic route to tert-butyloxycarbonylaminoacyl-4-(oxymethyl) phenylacetamidomethyl-resin, an improved support for solid-phase peptide synthesis, *J. Org. Chem.*, 1978, **43**(14), 2845–2852.
19 K. Kanie, K. Mizuno, M. Kuroboshi and T. Hiyama, A Facile Synthesis of Trifluoromethylamines by Oxidative Desulfurization-Fluorination of Dithiocarbamates, *Bull. Chem. Soc. Jpn.*, 1998, **71**(8), 1973–1991.
20 T. M. Hackeng, J. H. Griffin and P. E. Dawson, Protein synthesis by native chemical ligation: expanded scope by using

straightforward methodology, *Proc. Natl. Acad. Sci. U. S. A.*, 1999, **96**(18), 10068–10073.

21 M. A. Schnölzer, P. Alewood, A. Jones, D. Alewood and S. B. Kent, In situ neutralization in Boc-chemistry solid phase peptide synthesis, *Int. J. Pept. Protein Res.*, 1992, **40**(3–4), 180–193.

22 S. B. delCardayre and R. T. Raines, Structural determinants of enzymic processivity, *Biochemistry*, 1994, **33**(20), 6031–6037.

23 E. M. Crook, A. P. Mathias and B. R. Rabin, Spectrophotometric assay of bovine pancreatic ribonuclease by the use of cytidine 2′: 3′-phosphate, *Biochem. J.*, 1960, **74**(2), 234.

24 Z. Otwinowski and W. Minor, [20] Processing of X-ray diffraction data collected in oscillation mode, *Methods Enzymol.*, 1997, **31**(276), 307–326.

25 M. D. Winn, C. C. Ballard, K. D. Cowtan, E. J. Dodson, P. Emsley, P. R. Evans, R. M. Keegan, E. B. Krissinel, A. G. Leslie, A. McCoy and S. J. McNicholas, Overview of the CCP4 suite and current developments, *Acta Crystallogr., Sect. D: Biol. Crystallogr.*, 2011, **67**(4), 235–242.

26 R. A. Laskowski, M. W. MacArthur, D. S. Moss and J. M. Thornton, PROCHECK: a program to check the stereochemical quality of protein structures, *J. Appl. Crystallogr.*, 1993, **26**(2), 283–291.

27 A. Roussel and C. Cambillau, *Turbo-Frodo Manual*, AFMBCNRS, Marseille, France, 1996.

28 E. F. Pettersen, T. D. Goddard, C. C. Huang, G. S. Couch, D. M. Greenblatt, E. C. Meng and T. E. Ferrin, *J. Comput. Chem.*, 2004, **25**(13), 1605–1612.